

Radiocarbon Dating Bone Samples Recovered from Gravel Sites

Fiona Brock, Thomas Higham, and Christopher Bronk Ramsey

Summary

A range of pre-screening criteria which could be used on-site, in museums, or the laboratory were tested to determine which, if any, could be used to screen those suitable for radiocarbon dating prior to the time-consuming and costly collagen extraction pre-treatment chemistry.

Nearly 300 bones were analysed from 12 sites across southern England. The most successful screening method applied was the measurement of whole bone percent nitrogen. This method was consistently the most reliable predictor of suitability for radiocarbon dating. No other pre-screening criterion, or combination of criteria, showed a correlation with collagen preservation, either within the entire study or datasets from individual archaeological sites.

Keywords

Radiocarbon dating, bone

Authors' address

Oxford Radiocarbon Accelerator Unit, Research Laboratory for Archaeology & the History of Art, University of Oxford, Dyson Perrins Building, South Parks Road, Oxford, OX1 3QY

Introduction

Radiocarbon dating provides the backbone for most archaeological chronologies in the UK, particularly for the prehistoric period. The gravel terraces of our river valleys produce significant archaeological remains which often need to be dated. Bones, particularly those which articulate, are crucial to these chronologies as they provide substantial samples which relate directly to the context from which they were recovered.

However, many bones recovered from gravel sites in the UK have undergone severe chemical and physical degradation and subsequent microbial attack, resulting in greatly increased porosity and loss of up to 90% of the original collagen content. Such bones, therefore, have a relatively small possibility of containing sufficient collagen for reliable radiocarbon dating (ie more than 1% of the pristine amount) compared to bones from other contexts.

Radiocarbon pre-treatment chemistry is costly and time-consuming and so it is often not feasible to attempt to date bones, especially in large numbers, from gravel sites. However, sites which predominantly yield bone which contain insufficient surviving collagen to date do include a small fraction of bones in which collagen is better retained. The main aim of this project was to determine which, if any, analytical criteria could best be applied to gravel-deposited samples, and those from other sites known to yield poor bone preservation, either prior to their submission to the laboratory or during an initial screening process at the laboratory, to assess which bones might be successfully dated. Identification of any suitable diagnostic tests would make the dating of such sites more successful from a scientific standpoint, as well as faster and less costly.

Methods and Sampling

Samples of 298 human and animal bones (including *Sus scrofa*, *Bos primigenius*, *Bos taurus*, *Ovis aries*) were selected from 12 sites across southern England (Table 1). These were chosen to represent a range of contexts where bone preservation is thought to be poor or variable. A wide selection of bones, including femura, humeri, metacarpals, vertebrae, mandibula and scapulae, as well as antler, were sampled across a range of ages, from Neolithic to early medieval.

All of the bones were subjected to an initial screening process, which was designed to be used by archaeologists on-site or in museums. The criteria measured were:

- hardness
- colour (HSB: hue, saturation, brightness)
- dry bone bulk powder density
- microporosity.

Data from these bones was considered for scatter and range in the various measures. A total of 140 sub-samples were randomly selected and a further 60 selected judgementslly to cover specific cases missed in the random selection. These 200 bones were subjected to further diagnostic tests which could be carried out in the laboratory prior to pre-treatment for radiocarbon dating. These were:

- Fourier Transform Infra Red spectroscopy (FTIR)
- percent nitrogen and carbon analysis
- C:N atomic ratio of whole bone

The data produced for these bones was evaluated and half of the randomised samples (70) were selected again at random for full radiocarbon pre-treatment (using methods described

in Bronk Ramsey *et al.*, 2004). An additional 30 samples were chosen specifically to include those with as wide a range of values for the initial analyses as possible, although samples with very low nitrogen (<0.5%) were usually avoided as they were assumed to be unlikely to yield sufficient collagen for radiocarbon dating. The percentage yield of collagen, insoluble residue, and <30kD residue were calculated for each sample, and the stable isotopic values ($\delta^{13}\text{C}$, $\delta^{15}\text{N}$) and C:N atomic ratio of the purified collagen measured.

On the basis of the results observed throughout the study, 20 samples were selected for amino acid analysis, and 18 samples for small-angle X-ray scattering (SAXS) to represent samples with varying preservation states and from a range of sites.

Results

The results were studied to identify if any one, or any combination of, the diagnostic tests could be used to identify bones suitable for radiocarbon dating, and if any site specific trends could be observed. Details of the methods employed are provided in Appendix I; the data are provided in Appendices II and III.

Hardness: Hardness was measured using a modified Shore pencil durometer; the lower the value, the harder the bone. The hardness measurements ranged from 5 to 72 (arbitrary units) but failed to show any correlation with collagen preservation (Fig 1a). Some bones had very soft outer layers, and hence very high hardness values, but were actually much harder and well preserved under the surface. Other bones yielding low hardness values were simply brittle and poorly preserved. Several bones shattered on testing.

Colour: Neither hue, saturation, brightness, nor any combination of the three characteristics provided any indication of suitability for radiocarbon dating (Fig 1b). Bones tended to fall into several categories according to their colour following surface cleaning: those that became much darker (eg Fig 2a); those that were much lighter in colour beneath the surface (eg Fig 2b); and those that were unchanged (eg Figs 2c,d). Occasionally bones appeared to have several differently coloured layers beneath their surface. None of these observations provided any indication of collagen preservation.

Microporosity: Microporosity is defined as the volume of water uptake per gram of dried bone up to a relative humidity of 76%, which corresponds to all pores up to the theoretical diameter of 4nm being full of water. This has been suggested to be an indicator of bone diagenesis, as loss of protein has been observed to be reflected by both a loss in microporosity and an increase in crystallinity (Hedges *et al* 1995). Microporosity values in this study ranged from 0.07–0.19 cm^3g^{-1} , higher than the values of 0.025–0.105 cm^3g^{-1} reported from three archaeological sites by Hedges *et al.* (1995). This may be due to the small sample size used here, and by occasional inconsistencies in bone powder size (caused either by the use of different drill bits by different samplers or by fragmenting of the bone on sampling), but no correlation was observed between microporosity and the amount of collagen preserved in this study (Fig 1c).

Bulk powder density: These results may have been influenced by the same sample size issues as the microporosity samples, but again, no correlation between collagen preservation and bulk bone powder density was observed (Fig 1d). It should be noted that the bulk powder density values listed in this study of 0.24–0.52 gcm^{-3} are relative to each other, but that they may not be directly comparable to those in other published studies which analysed density of intact samples of bone. For example, Turner-Walker and Parry (1995) state that modern bone has a bulk density of $\sim 2.0 \text{ gcm}^{-3}$, and poorly preserved archaeological bone a bulk density of $\sim 0.8 \text{ gcm}^{-3}$.

FTIR: Modern bone normally contains 60–70% by weight of carbonated apatite crystals with a structure and composition similar to the mineral dahllite (Stiner *et al* 1995; Wright and Schwarz 1996). Infrared spectra of whole bone powder can provide both information on the crystallinity of the carbonate apatite crystals and a semi-quantitative estimate of the relative carbonate content of the mineral phase.

The crystallinity index or “splitting factor” (SF) of bone is calculated from the extent of splitting of the phosphate absorption peaks at $\sim 603\text{cm}^{-1}$ and 565cm^{-1} , as defined by Termine and Posner (1966) and Weiner and Bar-Yosef (1990). This represents a combination of both the relative sizes of the crystals and the extent to which the atoms are ordered within the lattice (Weiner and Bar-Yosef 1990).

During diagenesis, large crystals tend to grow at the expense of smaller ones, either rapidly over a period of a few months or years via weathering, or over many millennia during normal fossilization (Stiner *et al* 1995). Selective dissolution of more soluble, less ordered crystals may also occur in archaeological bones (Wright and Schwarz 1996). As recrystallization takes place, the two phosphate peaks become increasingly separated from each other, and this is reflected in the splitting factor: the higher the SF, the larger and/or the more ordered the crystals (Weiner and Bar-Yosef 1990).

Splitting factors of 2.5–2.9 have been recorded for fresh bones (Weiner and Bar-Yosef 1990; Stiner *et al* 1995; Sillen and Parkington 1996), and values of ~ 7 have been observed for highly fossilised or calcined bones (Weiner and Bar-Yosef 1990). All samples in this study had splitting factors of 3.6 and above, indicating that they were degraded to varying extents. There was no correlation in this study between splitting factor and percent collagen yield (Fig 3a).

The splitting factor is measured at the end of the spectrum, between ~ 500 and 750cm^{-1} and, in some cases, the spectrum was very poor and noisy, especially in the cases of very degraded bones. Despite baseline correction, this may have resulted in a slight elevation of the SF but not sufficiently to affect any correlation with collagen preservation. It should also be noted that SF has been observed to vary greatly throughout individual bones (Stiner *et al* 1995).

Carbonate content can be estimated from the ratio of the CO_3 and PO_4 absorbances at 1417cm^{-1} and 1035cm^{-1} respectively (Wright and Schwarz 1996). Loss of carbonate due to post-depositional recrystallization and hydroxyapatite alterations and/or burning results in lowering of the C:P ratio (Stiner *et al* 1995). The lower the C:P ratio, the more crystalline the bone.

Natural biogenic carbonate in bone has a C:P ratio of ~ 0.360 (Nielsen-Marsh, 1997 unpubl). In this study, C:P values ranged from 0.20 to 0.31, with the exception of 4 samples. These samples, 44 (from Eynesbury), 94, 97 (both from the Haddenham causewayed enclosure), and 175 (Etton causewayed enclosure) had C:P ratios of 0.61, 0.43, 0.34 and 0.33 respectively. Calcite peaks were observed at $\sim 710\text{cm}^{-1}$ in the FTIR spectra of all of these samples (but not in any other spectra) and may suggest growth of diagenetic calcite within the bone, especially for sample 44 (Eynesbury) The presence of calcite was reflected in the $\delta^{13}\text{C}$ of the whole bone, particularly for sample 44 which has the largest calcite peak and the most enriched $\delta^{13}\text{C}$ value of -11.7‰ (the majority of samples have $\delta^{13}\text{C}$ values which lie in the range -15 to -23‰). None of these samples were submitted for full radiocarbon pre-treatment, but they would all be expected to yield little collagen as none contained more than 0.2% nitrogen. All 5 samples with C:P ratios of 0.30 which were subjected to full pre-treatment yielded $>1\%$ collagen, but otherwise there was no correlation between C:P ratio and collagen preservation (Fig 3b).

Several studies have demonstrated that the relationship between C:P ratios and SF has reasonably good correlation with other pre-screening techniques (eg Petchey and Higham 2000). Sillen and Parkington (1996) also identified a very good correlation between SF and percent nitrogen in archaeological bones from one site in South Africa. In this study, there appears to be some correlation between samples with high SF (greater than ~ 4.8) and low C:P ratios (less than ~ 0.20) and preservation of collagen (Fig. 3c), but the relationship is not strong enough to use as a diagnostic test. Otherwise, no correlation within either the entire dataset or those of individual archaeological sites was found between C:P ratios and SF, or between either C:P or SF and any other pre-screening criteria.

Percent carbon and nitrogen analysis: Modern whole bone contains ~14% carbon (%C) (Sillen & Parkington, 1996). In this study, values ranged from 1.3 to 12.0% and all samples with 7.2% C and above yielded > 1% weight collagen and were therefore suitable for radiocarbon dating (Fig. 4a). However, there was no significant correlation between % weight collagen and %C, as the technique cannot distinguish between carbon present in collagen or contaminant.

Percent nitrogen (%N) values for whole bone provide an indication of protein survival as nitrogen in bone is derived solely from the proteinaceous component. %N can be used to indicate whether or not there is sufficient collagen in the bone for radiocarbon dating to be successful. The value will not, however, identify whether the nitrogen is present as collagen or as contaminants, nor will it specify the amount of non-nitrogenous soil-derived organic matter present (Hedges and van Klinken 1992).

Fresh bone contains ~ 4% nitrogen (Stafford *et al* 1988; Ambrose 1993). In this study, the maximum nitrogen detected was 3.7% (sample 210, Cleveland Farm). All samples with more than 2% nitrogen which underwent pre-treatment yielded sufficient collagen for AMS radiocarbon dating (2.4–6.5% wt collagen) but the majority of samples contained 1% nitrogen or less (Fig. 4b).

However, of the pre-screening techniques investigated in this study, %N of whole bone was the most reliable tool for identifying samples with sufficient collagen for radiocarbon dating. Linear regression analysis demonstrated that if 0.76% N is chosen as the threshold, 84% of those bones will be correctly identified as dateable or not dateable (Fig. 4b). Where C = % weight collagen and N = % nitrogen of whole bone:

$$C_{\text{pred}} = a + bN$$

(a = -0.02 ± 0.15, b = 1.36 ± 0.12 and R = 0.759).

Inclusion of the %C and/or the C:N atomic ratio of bone in the linear regression increased the prediction success to 85%, which is not significantly better.

C:N atomic ratio of whole bone: The C:N atomic ratio of whole bone can provide an indication of the general state of preservation of the collagen, the extent to which deamination has taken place and/or the extent of contamination by exogenous carbon-containing compounds such as humic acids (Tisnérat-Laborde *et al* 2003). A C:N ratio of greater than 5 demonstrates extensive diagenesis and/or the presence of a high proportion of humics (Tisnérat-Laborde *et al* 2003).

Samples within this study produced C:N atomic ratios of 3.6–98.1, although only 16% of the 200 samples analysed had ratios less than 5. In general, this study suggests that bones with C:N ratio of greater than ~6.5–7.0 are not suitable for radiocarbon dating, but one sample (number 126, Berinsfield) yielded 1.1% wt collagen on pre-treatment with a C:N ratio of 8.7 (Fig. 4c).

Full radiocarbon pre-treatment: Modern fresh bone typically contains ~ 22% wt collagen (van Klinken 1999). At the Oxford Radiocarbon Accelerator Unit, samples yielding less than 1% wt collagen after full pre-treatment are failed and not submitted for AMS dating. Of the 100 samples which underwent full radiocarbon pre-treatment, only 45 yielded greater than 1% wt collagen and were therefore deemed suitable for dating (Table 2).

The bones from Berinsfield generally demonstrated good preservation, as did those from Holloway Lane and Bestwall Quarry. It should be noted that the differing yields of collagen between samples from Berinsfield recorded in this study and those published by Privat *et al* (2002) are most likely due to differences in pre-treatment procedures: Privat *et al* used only an acid wash prior to gelatinization, and did not include the base wash and ultrafiltration utilized in this study and currently as standard for radiocarbon dating at the Oxford Radiocarbon Accelerator Unit (Bronk Ramsey *et al* 2004).

No samples from either Eynesbury or Haddenham Causewayed Enclosure contained sufficient collagen for dating, but this was unsurprising as all of the 40 samples analysed contained low levels of nitrogen.

C:N ratios of collagen are typically 2.9–3.6 (DeNiro 1985). Values out of this range are indicative of low collagen (Schoeninger *et al* 1989; Ambrose 1990), contamination (DeNiro 1985; Ambrose 1990) or diagenesis (Koch *et al* 1994). At the Oxford Radiocarbon Accelerator Unit, our cut-off for dating is 2.9–3.5.

All but four bones in this study had collagen with a C:N atomic ratio of 3.2 or 3.3, regardless of the amount of collagen preserved. One sample (number 35, Holloway Lane) had a C:N ratio of 2.9 and yielded 1.9% wt collagen, two samples (numbers 178 and 179, both from Etton causewayed enclosure) had C:N ratios of 3.4 and yielded 0.9% and 0.5% wt collagen respectively, and sample 182 (also from Etton) had a ratio of 86.4 due to very low nitrogen and yielded only 0.5% wt collagen.

Stable isotopic values ($\delta^{13}\text{C}$ and $\delta^{15}\text{N}$) of collagen are more likely to be linked to sample-specific variables (eg trophic-level in herbivores or carnivores in $\delta^{15}\text{N}$) and environmental influences (eg $\delta^{13}\text{C}$ canopy effects in forests) than collagen preservation (van Klinken 1999).

The amount of insoluble residue present after radiocarbon pre-treatment ranged from 0 to 42% (Fig. 4d) and varied greatly within archaeological sites. The percentage of material which passed through the ultrafilter during pre-treatment (ie < 30 kDa residue) reached a maximum of 1.6%, although the residue was often very sticky and difficult to weigh. Neither residue correlated with the percent weight collagen yielded for a given sample.

Amino acid analysis: allows the detailed composition of the proteins present to be determined and compared to those of collagen in modern bone (van Klinken 1999). However, for the majority of bones, there is little actual variation in the amino acid profiles themselves, it is only when the bones become very degraded that reduced levels of certain amino acids are present (van Klinken 1999). One of the limitations of amino acid analysis in this study was that there was insufficient collagen for the analysis to be carried out on many of the samples which failed pre-treatment.

Of the 20 collagen samples analysed, five were from bones which had yielded less than 1% wt collagen. It was not easy to distinguish these specific samples from those that were successful in pre-treatment using their amino acid profiles, except for sample number 182 (Etton) for which the pre-treatment product was a brown powder. This sample had reduced levels of hydroxyproline, proline, glycine, and alanine in comparison with the other collagen samples. Sample 280 (RMC Land), which also failed pre-treatment and which appeared brittle and glassy, was only differentiated from the other samples by slightly reduced alanine levels. Of the other samples with low collagen yields, sample 127 (Berinsfield) demonstrated

slightly reduced levels of alanine and aspartic acid, but samples 178 and 179 (Etton) were indistinguishable by their amino acid profiles from the samples with good collagen preservation.

Several studies have attempted to use ratios of various amino acids to categorise collagen preservation (eg Stafford *et al* 1988; DeNiro and Weiner 1988; Weiner and Bar-Yosef 1990). It was nearly impossible to assign any of the 20 bones sampled to the classes of preservation defined by Stafford *et al* (1988) on the basis of their amino acid profiles and whole bone percent nitrogen content. Sample 182 could clearly be assigned to class V (“extremely poorly preserved”), but most other bones could only be attributed to combined classes I–III (“modern”, “very well to well preserved”, and “moderately well preserved” respectively) using these criteria.

Weiner and Bar-Yosef (1990) used Gly/Asp ratios (glycine/aspartic acid ratios) to determine collagen purity: pure collagen has a Gly/Asp ratio of close to 7 (Weiner and Bar-Yosef 1990). They stated that collagen is not present in samples with a Gly/Asp ratio of less than ~ 6. However, in this study, sample 99 (Berinsfield) has a ratio of 5.6 but yielded 2.5% wt collagen with a C:N ratio of 3.2 and $\delta^{13}\text{C}$ of -20.2‰ , suggesting that it was not affected by contamination. Most of the other samples had Gly/Asp ratios of 6.4–7.5, except two with poor collagen preservation, samples 127 (Berinsfield) and 182 (Etton) with ratios of 8.2 and 30.9 respectively.

DeNiro and Weiner (1988) used several amino acid ratios - Asp/Pro (aspartic acid/proline), Asp/Gly (aspartic acid/glycine), and Asp+Thr+Ser+Glu/Pro+Gly+Hop ((aspartic acid + threonine + serine + glutamic acid)/(proline + glycine + hydroxyproline)) - to distinguish between modern, well-preserved, and poorly-preserved prehistoric bones. With the exception of sample 182, there is little variation between these ratios among the samples in this study, and all have ratios which agree with those of DeNiro and Weiner’s modern and well-preserved samples.

Small-angle X-ray scattering (SAXS): This technique allows for the accurate measurement of crystal shape, size, and orientation within bone and has been used to determine the degree to which the bone matrix has recrystallised (Wess *et al* 2001; Hiller *et al* 2004; Hiller and Wess 2006). Hiller *et al* (2004) and Hiller and Wess (2006) used the method to study the structural dimensions of crystallites in bones and demonstrated a link between alteration to crystal structure (in terms of thickness or shape) and other diagenetic changes such as loss of nitrogenous material. In this study, 18 samples were analysed using SAXS, but no correlation between crystal thickness and collagen preservation was observed (Fig 3d).

Interpretation and conclusions

Of the pre-screening criteria tested in this study, only %N (and, to a lesser extent, %C and C:N atomic ratio) of whole bone showed a good correlation with collagen preservation which could be applied to bone specimens to identify those suitable for radiocarbon dating. Linear regression analysis demonstrated that using a 0.76% N cut-off level would allow an 84% prediction rate for whether a bone was dateable or not. This prediction success was increased to 85% when including the %C and/or C:N atomic ratio data in the linear regression.

Percent nitrogen analysis of bone powder is a relatively quick and simple technique and could easily be implemented as a pre-screening technique prior to radiocarbon dating of bone samples from sites known to suffer from poor or variable preservation such as Brandon Staunch Meadow, Etton Causewayed Enclosure, and Kingsmead Quarry. This level of nitrogen is less than the 1% cut-off currently used at the Oxford Radiocarbon Accelerator

Unit to determine whether or not to proceed with pre-treatment of potentially poorly preserved bones.

No correlation between any of the pre-screening criteria and % weight collagen was observed within any of the individual archaeological sites studied.

Acknowledgements

The authors wish to thank everyone who provided material for this study and assisted with the laboratory work: Alex Bayliss, John Meadows, Derek Hamilton, and Wendy Hart (English Heritage); Angela Bowles, Christine Tompkins, Jane Davies, and Barbara Emery (Oxford Radiocarbon Accelerator Unit) for sampling the bones and full radiocarbon pre-treatment; Peter Ditchfield (Oxford Radiocarbon Accelerator Unit) for stable isotope analysis; Tony Willis (Department of Biochemistry, University of Oxford) for amino acid analysis; Colin Johnston and Alison Crossley for permission to use, and assistance with, FTIR at the Department of Materials, University of Oxford and BegbrokeNano (supported by the DTI MNT Capital Programme); Clerk Maxwell and Tim Wess (Cardiff University) for SAXS, and Jen Hiller (Diamond Synchrotron) for analysis of the data.

We are grateful to the following who kindly provided bone specimens for this study: Andrew Tester, Suffolk County Council (Brandon Staunch Meadow); Nick Elsdon, Museum of London Archaeology Service (Holloway Lane); Quinton Carroll, Cambridgeshire County Council (Eynesbury); Chris Evans, Cambridge Archaeological Unit, University of Cambridge (Haddenham Causewayed Enclosure); Dr Andrew Chamberlain, University of Sheffield (Wally Corner, Berinsfield); Robin Jackson, Worcestershire County Council (Huntsman's Quarry); Lilian Ladle, Bestwall Quarry archaeology project; Dr Frances Healy, Cardiff University (Etton causewayed enclosure); Lorraine Mephram, Wessex Archaeology (Imperial College Sports Ground, Cleveland Farm, Kingsmead Quarry, RMC Land).

References

- Ambrose, S H, 1990 Preparation and characterisation of bone and tooth collagen for isotopic analysis, *Journal of Archaeological Science*, **17**, 431–51
- Ambrose, S H, 1993 Isotopic analysis of paleodiets: methodological and interpretive considerations, in *Investigations of ancient human tissue* (ed M K Sandford), 59–130, Amsterdam (Gordon and Breach Science Publishers)
- Bronk Ramsey, C, Higham, T, Bowles, A, and Hedges, R E M, 2004 Improvements to the pre-treatment of bone at Oxford, *Radiocarbon*, **46**, 155–64
- DeNiro, M J 1985 Postmortem preservation and alteration of *in vivo* bone collagen isotope ratios in relation to palaeodietary re-construction, *Nature*, **317**, 806–9
- DeNiro, M J, and Weiner, S, 1988 Chemical, enzymatic and spectroscopic characterization of “collagen” and other organic fractions from prehistoric bones, *Geochimica et Cosmochimica Acta*, **52**, 2197–2206
- Hedges, R E M, and van Klinken, G J, 1992 A review of current approaches in the pre-treatment of bone for radiocarbon dating by AMS, *Radiocarbon*, **34**, 279–91
- Hedges, R E M, Millard, A, and Pike, A W G, 1995 Measurements and relationships of diagenetic alteration of bone from three archaeological sites, *Journal of Archaeological Science*, **22**, 201–9
- Hiller, J C, Collins, M J, Chamberlain, A T, and Wess, T J, 2004 Small-angle X-ray scattering: a high-throughput technique for investigating archaeological bone preservation, *Journal of Archaeological Science*, **31**, 1349–59
- Hiller, J C, and Wess, T J, 2006 The use of small-angle X-ray scattering to study archaeological and experimentally altered bone, *Journal of Archaeological Science*, **33**, 560–72
- Koch, P L, Fogel, M L, and Tuross, N, 1994 Tracing the diets of fossil animals using stable isotopes. In (K Lajtha and B Michener, Eds) *Stable Isotopes in Ecology and Environmental Science*. Oxford: Blackwell Scientific Publications, pp 63-92.
- Nielsen-Marsh, C, 1997 unpubl Studies in archaeological bone diagenesis, PhD thesis, Univ Oxford
- Petchey, F, and Higham, T, 2000 Bone diagenesis and radiocarbon dating of fish bones at the Shag River Mouth Site, New Zealand, *Journal of Archaeological Science*, **27**, 135–50
- Pike, A W G, 1993 unpubl Bone porosity, water and diagenesis: towards a grand unifying theory of bone diagenesis, Part II Undergraduate dissertation, Univ Bradford
- Privat, K P, O’Connell, T C, and Richards, M P, 2002 Stable isotope analysis of human and faunal remains from the Anglo-Saxon cemetery at Berinsfield, Oxfordshire: dietary and social implications, *Journal of Archaeological Science*, **29**, 779–90
- Schoeninger, M J, Moore, K M, Murray, M L, and Kingston, J D, 1989 Detection of bone preservation in archaeological and fossil samples, *Applied Geochemistry*, **4**, 281–92
- Sillen, A, and Parkington, J, 1996 Diagenesis of bones from Eland’s Bay Cave, *Journal of Archaeological Science*, **23**, 535–42

Stafford Jr, T W, Brendel, K, and Duhamel, R C, 1988 Radiocarbon, ^{13}C and ^{15}N analysis of fossil bone: removal of humates with XAD-2 resin, *Geochimica et Cosmochimica Acta*, **52**, 2257–67

Stiner, M C, Kuhn, S L, Weiner, S, and Bar-Yosef, O, 1995 Differential burning, recrystallization, and fragmentation of archaeological bone, *Journal of Archaeological Science*, **22**, 223–37

Termine, J D, and Posner, A S, 1996 Infrared analysis of rat bone: age dependency of amorphous and crystalline mineral fractions, *Science*, **153**, 1523–5

Tisnérat-Laborde, N, Valladas, H, Kaltnecker, E, and Arnold, M, 2003 AMS radiocarbon dating of bones at LSCE, *Radiocarbon*, **45**, 409–19

Turner-Walker, G, and Parry, T V, 1995 The tensile strength of archaeological bone, *Journal of Archaeological Science*, **22**, 185–91

van Klinken, G J, 1999 Bone collagen quality indicators for palaeodietary and radiocarbon measurements, *Journal of Archaeological Science*, **26**, 687–95

Weiner, S, and Bar-Yosef, O, 1990 States of preservation of bones from prehistoric sites in the Near East: a survey, *Journal of Archaeological Science*, **17**, 187–96

Wess, T J, Drakopoulos, M, Snigirev, A, Wouters, J, Paris, O, Fratzl, P, Collins, M, Hiller, J, and Nielsen, K, 2001 The use of small-angle X-ray diffraction studies for the analysis of structural features in archaeological samples, *Archaeometry*, **43**, 117–29

Wright, L E, and Schwarcz, H P, 1996 Infrared and isotopic evidence for diagenesis of bone apatite at Dos Pila, Guatemala: palaeodietary implications, *Journal of Archaeological Science*, **23**, 933–44

Table 1. Details of the 12 sites from southern England from which bones were sampled for this study

Site Name	Location	Age of Bones
Brandon Staunch Meadow	Suffolk	Anglo-Saxon, early medieval
Holloway Lane, Harmondsworth	London Borough of Hillingdon	Pre-historic multi-period site, especially late Neolithic-early Bronze Age
Eynesbury	Barford Road, St Neots, Cambs.	Neolithic, from Neolithic to Anglo-Saxon site
Haddenham Causewayed Enclosure	Haddenham, Cambs.	Early Neolithic features, from multi-period site
Wally Corner, Berinsfield	Dorchester-on-Thames, Oxon	Anglo-Saxon cemetery
Huntsman's Quarry	Kemerton, Worcestershire	Late Bronze Age features, from multi-period site
Bestwall Quarry	Wareham, Dorset	Bronze Age, Romano-British, Anglo-Saxon
Etton Causewayed Enclosure	Maxey, nr Peterborough, Cambs.	Early Neolithic
Imperial College Sports Ground, Harlington	London Borough of Hillingdon	Romano-British
Cleveland Farm	Ashton Keynes, Wiltshire	Iron Age or Romano-British
Kingsmead Quarry, Horton	Windsor & Maidenhead, Berks.	Bronze Age
RMC Land, Harlington	London Borough of Hillingdon	Bronze Age, Romano-British, Anglo-Saxon

Table 2. Collagen yields for samples which underwent full radiocarbon pre-treatment

Site	No. bones sampled	No. bones pre-treated	No. bones >1% collagen	% bones >1% collagen
Brandon Staunch Meadow	30	8	4	50
Holloway Lane	12	4	3	75
Eynesbury	18	4	0	0
Haddenham Causewayed Encl.	43	10	0	0
Wally Corner, Berinsfield	31	16	13	81
Huntsman's Quarry	25	7	2	29
Bestwall Quarry	13	9	9	100
Etton Causewayed Encl.	18	7	3	43
Imperial College Sports Ground	20	5	1	20
Cleveland Farm	28	10	4	40
Kingsmead Quarry	30	7	1	14
RMC Land, Harlington	30	13	5	38
Total	298	100	45	45

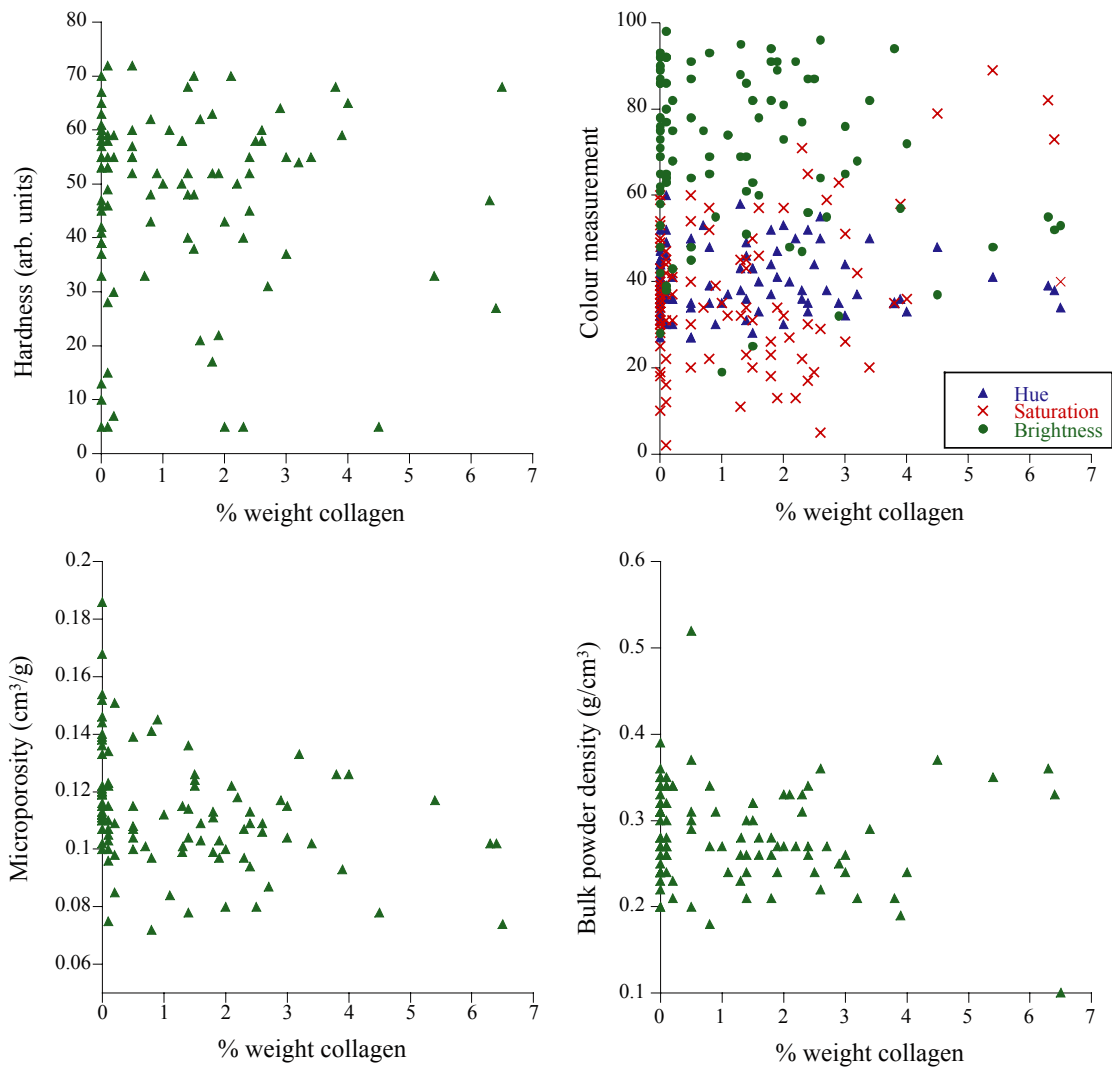


Figure 1. Plots of a) hardness, b) colour measurement (hue, saturation, and brightness), c) microporosity, and d) bulk powder density against % weight collagen

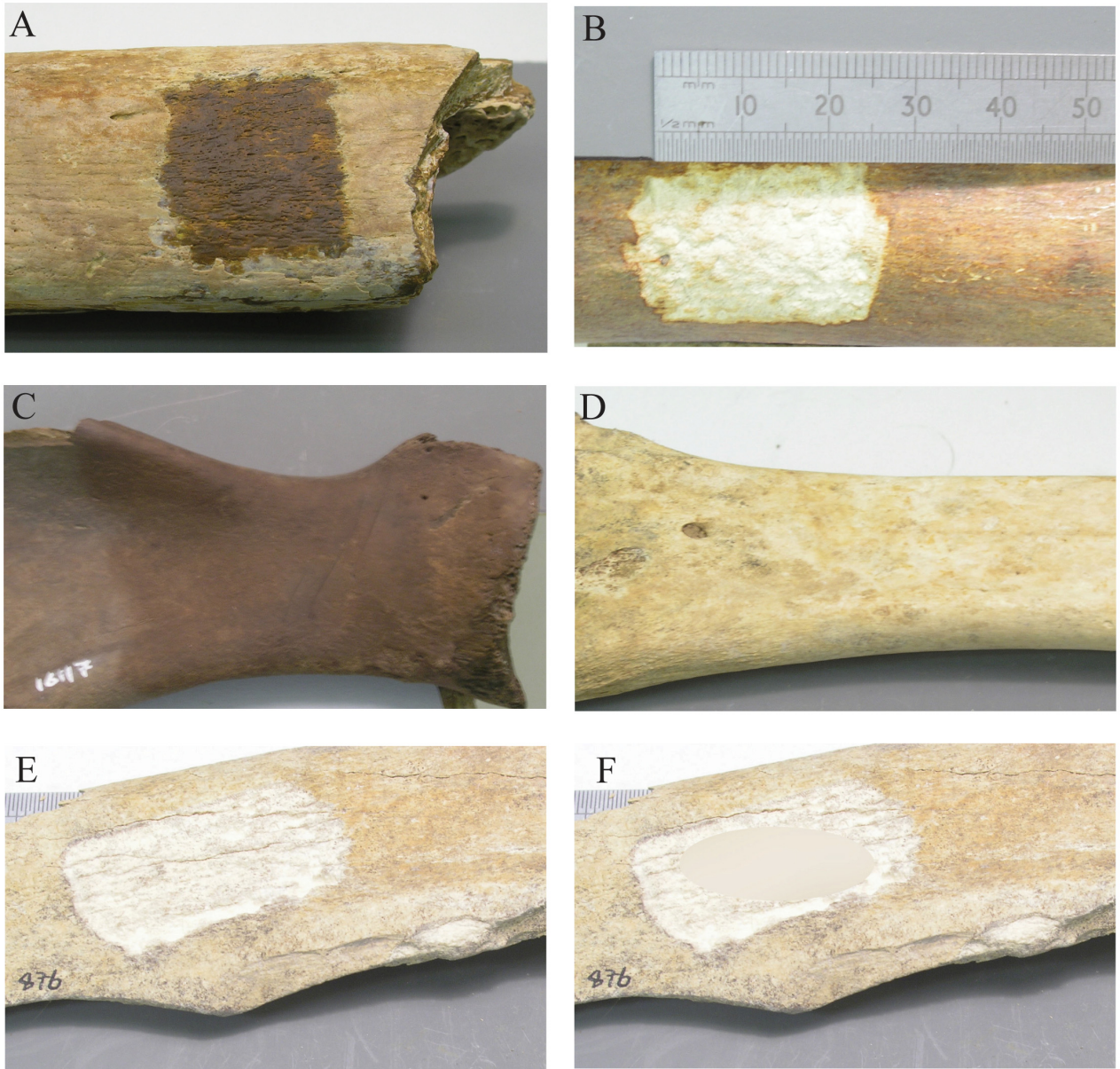


Figure 2: Examples of the variation in appearance of bone and the effect of cleaning the bone surface by shotblasting. Hue (H), saturation (S) and brightness (B) values varied accordingly: A) Sample 60 (Eynesbury) H: 31, S: 37, B: 41; B) Sample 123 (Mount Farm) H: 58, S: 11, B: 91; C) Sample 175 (Etton) H: 25, S: 34, B: 45; D) Sample 282 (RMC Land, Harlington) H: 46, S: 26, B: 90; E) Sample 265 (RMC Land, Harlington) H: 47, S: 8, B: 93; F) Sample 265 showing area of Gaussian blur averaging used to measure HSB.

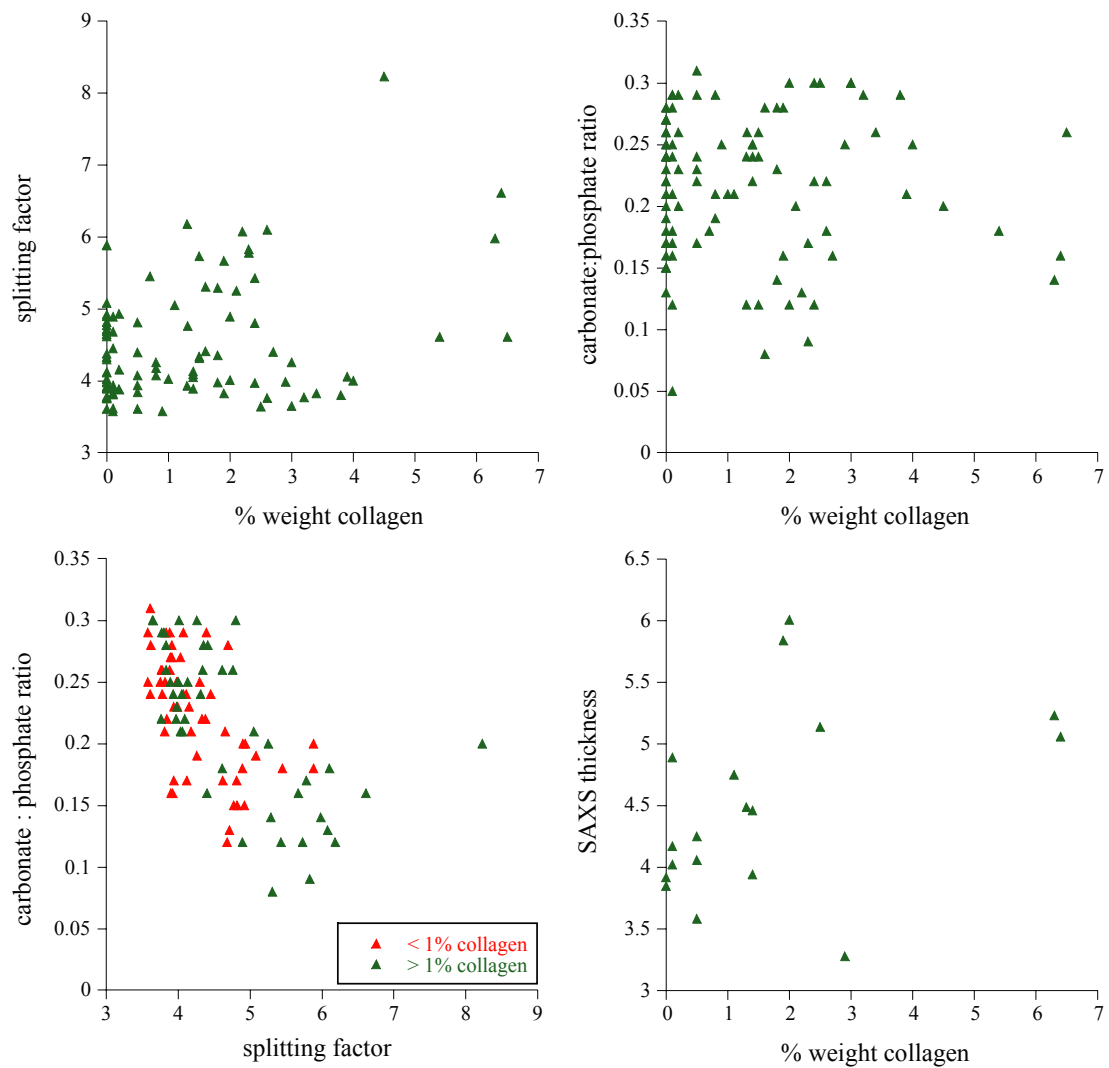


Figure 3. Plots of a) splitting factor (SF) and b) carbonate : phosphate ratio (C:P) against % weight collagen; c) splitting factor vs carbonate : phosphate ratio; d) SAXS crystallinity thickness against % weight thickness

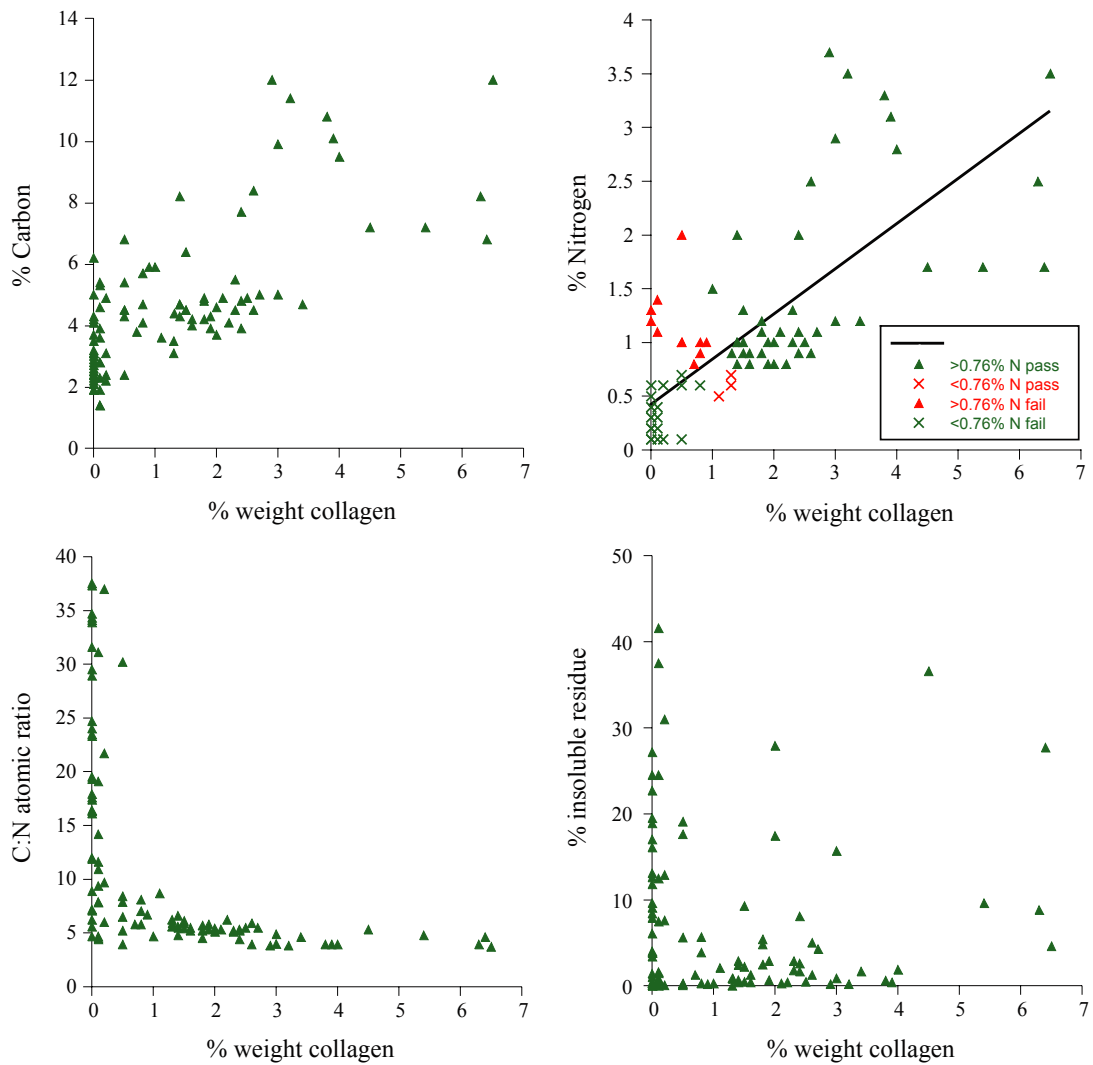


Figure 4. Plots of a) % carbon, b) % nitrogen, showing the line of linear regression and indicating those which “passed” and “failed” radiocarbon treatment (ie those with yields of >1% and <1% weight collagen respectively). Samples which are correctly predicted to pass or fail radiocarbon pre-treatment are in green, and those which are incorrectly predicted in red; c) C:N atomic ratio of whole bone, and d) % insoluble residue against % weight collagen

Appendix I: Methods

Hardness: An Intron Shore Pencil Durometer was used to measure hardness of a bone by determining the depth of penetration of an indenter into the bone. The durometer was modified to require 5kg to fully compress the spring, and the origin blunt indenter was sharpened to a 60° angle. Three closely-spaced measurements were taken from a flat portion of the bone (where possible), and the average of the three values calculated. The units are arbitrary.

Colour: Each bone was shot-blasted with fine aluminium oxide powder (Swan-Blaster, Crystal Mark Inc, Glendale CA, USA; Airbrasive powder No. 1, REG Abrasives Ltd, Dartford, UK) to remove surficial contamination before being digitally photographed against a Kodak grey card background. The image was adjusted for grey-point and HSB (hue, saturation, brightness) were measured over a sample area using Gaussian blur averaging in Adobe Photoshop software.

Sampling: The cleaned section of the bone was drilled using a tungsten carbide spherical burr drill bit (3mm diameter) at a low speed, and ~1g bone powder collected. For consistency the same bit and speed was used where possible within the Oxford Radiocarbon Accelerator Unit, although this was not always possible for bones sampled elsewhere.

Microporosity: 20–30mg bone powder was transferred to a 4mL Wheaton vial of known weight. Samples were oven-dried at 100°C for a minimum of three days prior to weighing. The samples were then transferred to a thermostatically-controlled humidity chamber at 25°C with at 75% relative humidity (RH). Humidity was controlled using sulphuric acid and measured with a hygrometer (Pike 1993 unpubl). Samples were left for 3 days prior to weighing. Each weight measurement was repeated 3 times and an average calculated. Microporosity was calculated as follows:

$$\text{Microporosity} = \frac{75\% \text{ RH weight} - \text{oven dry weight}}{\text{oven dry weight}}$$

according to Nielsen-Marsh (1997 unpubl).

Bulk powder density: The samples which had been weighed out for microporosity measurements were dried in an oven at 100°C for at least three days and then allowed to cool over silica gel in a dessicator. A 1.5mm micro-curette with an approximate volume of 1.77mm³ was used to weigh out three aliquots of dried bone powder. For each aliquot, the micro-curette was loaded up with bone powder which was pressed down against the side of the vial. The micro-curette was then tapped three times to remove excess or loose powder, before the surface of the bone powder was levelled off using a clean scalpel. The average of the three weights was calculated and divided by 1.77 to calculate the bulk powder density. Note that such a small volume was required due to the limited amount of bone powder available, and that the values for should be taken as relative to each other, but not absolute due to uncertainty of the volume of the micro-curette. As for the microporosity measurements, bulk powder density could not be calculated for samples which had fragmented on drilling due to heterogeneous grain size.

FTIR: Infra-red spectra of bone powder was obtained using Varian Excalibur series FTIR with a Specac Golden Gate ATR at BegbrokeNano, part of the Department of Materials, Oxford University. Data was manipulated and measured using Digilab Resolutions Pro 4.0 software. Each sample was run in triplicate for 20 scans and each spectrum subject to background subtraction and baseline correction. The splitting factor (SF), or crystallinity index, was calculated for each spectrum according to Weiner and Bar-Yosef (1990) as follows:

$$\text{SF} = \frac{\text{height of peak at } 603\text{cm}^{-1} + \text{height of peak at } 565\text{cm}^{-1}}{\text{distance from the baseline to the trough between the 2 peaks}}$$

when the baseline was drawn between 500 and 750 cm^{-1} .

The carbonate : phosphate ratio (C:P) was calculated according to Wright and Schwarcz (1996) as:

$$\text{C:P} = \frac{\text{height of carbonate peak at } 1417 \text{ cm}^{-1}}{\text{height of phosphate peak at } 1022 \text{ cm}^{-1}}$$

Both SF and C:P were calculated for all three spectra for each sample and averaged.

Elemental analysis: %C, %N, and C:N atomic ratio.

Whole bone and collagen samples were analysed using an automated carbon and nitrogen elemental analyser (Carlo Erba EA1108) coupled with a continuous-flow isotope ratio-monitoring mass spectrometer (Europa Geo 20/20).

Full radiocarbon pre-treatment: The method is detailed by Bronk Ramsey *et al* (2004).

Briefly:

- coarsely ground bone powder (~600mg) was sequentially treated with hydrochloric acid (0.5M), sodium hydroxide (0.1M), and hydrochloric acid (0.5M) with thorough rinsing with ultrapure (MilliQ™) water between each reagent;
- crude collagen was then gelatinized in pH3 solution at 75°C for 20 hours;
- the gelatin solution was filtered using a 9 μm polyethylene Eezi-filter™ which had been cleaned by ultrasonication in ultrapure water for 20 minutes;
- the filtered gelatin was transferred into a pre-cleaned ultrafilter (Vivaspin™ 15 30 kD MWCO) and centrifuged at 2500–3000 rpm until 0.5–1.0mL of the > 30 kD gelatin fraction remained (typically 20–40 minutes);
- this fraction was freeze-dried and the resulting purified collagen weighed.

During this procedure, both the insoluble residue left after Eezi-filtering and the gelatin which passed through the ultrafilter were freeze-dried and weighed, and the percentage insoluble residue and < 30 kD component calculated respectively. The percent collagen yield was also calculated in relation to the starting weight of the bone powder.

The stable isotopic values ($\delta^{13}\text{C}$, $\delta^{15}\text{N}$) and C:N ratio of the collagen was measured as for the whole bone powder.

Amino acid analysis: Analysis was carried out by Tony Willis at the MRC Immunochemistry Unit in the Department of Biochemistry, University of Oxford. 2.5 nanomoles of an internal standard mixture of nor-valine and sarcosine was added to each sample of purified collagen (~1 mg) and samples were dried in pyrolysed Pyrex tubes (Corning 9820 culture tubes) before being hydrolysed in vapour-phase for 22 hours at 110°C. The hydrolysing medium was 5.7N hydrochloric acid (constant boiling) with a trace of phenol added. Amino acid analysis was performed using an Agilent 1100 series HPLC with a G1327A autosampler and G1321A fluorescence detector. Samples were derivitised with ortho-phthalaldehyde (OPA) for the primary amino acids and 9-fluorenylmethyl chloroformate (FMOC) for the secondary amino acids. 1 μl of redissolved hydrolysate was injected onto a Hypersil AA-ODS HPLC column (Agilent) to resolve the derivitised amino acids. Results were integrated using Agilent ChemStation software with three point calibration in each batch of samples using standard runs of 10, 25, and 100 picomoles, and are given as mole %.

SAXS: Analysis was carried out by Clerk Maxwell in the School of Optometry and Vision Sciences, Cardiff University. Bone powder (~ 15mg) was loaded into a specially designed sample carriage between two mica sheets. This was attached to a sample stage which was mounted into the vacuum chamber of the NanoSTAR (Bruker AXS, Karlsruhe) X-ray facility.

The SAXS configuration uses a sample-to-detector distance of 1.25m. Bone scattering profiles typically require 3-hour exposures. Data is collected according to Wess *et al* (2001), corrected for camera distortions, subjected to ultralene background subtraction, and images analysed using in-house software. The two-dimensional detector output is converted into spherically averaged one-dimensional profiles, and values for crystal thickness determined.

Appendix II: Data

ID	Site	Site ID	Hardness		Colour		Micro-porosity cm ³ /g	Bulk powder density g/cm ³	Whole bone powder			Splitting factor	Carbonate: phosphate	Radiocarbon pre-treatment			Collagen			SAXS Ave thickness nm		
			arb. unit	Hue	Saturation	Brightness			%N	%C	C/N			% ^{δ¹³C}	% ^{δ¹⁵N}	% ^{δ¹³C}	% ^{δ¹⁵N}	% ^{δ¹³C}	% ^{δ¹⁵N}		No reps	% ^{δ¹³C}
1	Brandon Staunch Meadow	1708	55	36	48	68	0.083	0.31	-24.32	0.2	3.2	17.6	5.06	0.16								
2	Brandon Staunch Meadow	1779	53	36	52	67	0.088	0.19														
3	Brandon Staunch Meadow	1803	59	36	58	57	0.093	0.19	-19.95	3.1	10.1	3.9	4.06	0.21	0.4	0.1	3.9	-19.63	10.85	3.2		
4	Brandon Staunch Meadow	1816	59	33	52	67	0.086	0.22	-23.46	1.2	5.7	5.7	4.31	0.18								
5	Brandon Staunch Meadow	1830	47	33	42	67	0.080	0.18														
6	Brandon Staunch Meadow		27	39	52	78																
7	Brandon Staunch Meadow	1838	58	35	54	66	0.071	0.23	-20.10	1.0	4.8	5.7	4.32	0.18								
8	Brandon Staunch Meadow	1850	29	38	56	66	0.071	0.28	-27.48	0.3	4.2	17.6	4.51	0.19								
9	Brandon Staunch Meadow	1861	62	35	52	65	0.072	0.18	-21.98	1.0	5.7	7.0	4.18	0.21	5.7	0.1	0.8	-19.76	10.32	3.3		
10	Brandon Staunch Meadow	1863	68	34	40	53	0.074	0.10	-18.91	3.5	12.0	3.7	4.61	0.26	4.6	0.0	6.5	-19.50	10.10	3.2		
11	Brandon Staunch Meadow	1882	61	35	53	66	0.114	0.24	-19.44	2.1	7.7	4.2	4.58	0.22								
12	Brandon Staunch Meadow	1898	55	39	47	78	0.113	0.29														
13	Brandon Staunch Meadow	1900	55	35	54	64	0.107	0.37	-22.36	0.6	4.3	8.4	4.81	0.17	5.6	0.1	0.5	-19.63	9.94	3.3		
14	Brandon Staunch Meadow	1917	51	34	53	58	0.097	0.43														
15	Brandon Staunch Meadow	1919	33	42	44	82	0.108	0.27	-21.61	0.7	4.4	7.5	4.79	0.17								
16	Brandon Staunch Meadow	1923	52	37	50	72	0.081	0.35														
17	Brandon Staunch Meadow	3067	48	39	57	69	0.097	0.34	-20.77	0.9	4.7	5.8	4.26	0.19	3.9	0.0	0.8	-19.32	10.55	3.3		
18	Brandon Staunch Meadow	3081	28	35	54	61	0.092	0.22	-19.69	3.5	11.5	3.9	5.06	0.26								
19	Brandon Staunch Meadow	3082	55	35	54	65	0.096	0.30	-20.90	1.3	5.7	5.2	4.23	0.18								
20	Brandon Staunch Meadow	3090	57	32	45	47	0.090	0.32														
21	Brandon Staunch Meadow	3103	55	32	51	65	0.115	0.24	-19.32	2.9	9.9	4.0	4.26	0.30	0.9	0.1	3.0	-19.26	9.33	3.2		
22	Brandon Staunch Meadow	3112	60	33	51	67	0.110	0.14														
23	Brandon Staunch Meadow	3113	58	37	56	66	0.109	0.20	-19.08	3.7	11.3	3.6	4.29	0.24								
24	Brandon Staunch Meadow	3127	62	38	51	65	0.100	0.20														
25	Brandon Staunch Meadow	3136	68	36	45	61	0.104	0.21	-20.67	2.0	8.2	4.8	4.05	0.24	2.9	0.1	1.4	-20.19	9.69	3.3		
26	Brandon Staunch Meadow	4009	58	36	56	64	0.101	0.24														
27	Brandon Staunch Meadow	4035	58	31	45	48			-19.41	3.2	10.4	3.8	4.48	0.26								
28	Brandon Staunch Meadow	4042	50	38	51	78	0.093	0.18														
29	Brandon Staunch Meadow	4054	49	36	47	65	0.096	0.26	-23.22	0.3	3.9	14.2	4.89	0.18	1.6	0.0	0.1					
30	Brandon Staunch Meadow	8007	60	34	55	57	0.084	0.21														
31	Holloway Lane	HL 87 B1	47	36	16	89	0.100	0.18	-19.87	0.4	2.7	8.3	4.68	0.14								
32	Holloway Lane	HL 87 B14	17	37	18	82	0.111	0.21	-22.38	1.2	4.8	4.5	5.29	0.14	4.8	0.4	1.8	-24.00	7.91	3.2		
33a	Holloway Lane	HL 87 B62		36	28	78	0.111	0.18														
33b	Holloway Lane	HL 87 B62b		34	26	78																
34	Holloway Lane	HL 87 B65	47	34	32	75	0.107	0.30	-25.08	1.5	5.1	4.0	5.64	0.16								
35	Holloway Lane	HL 87 B66	22	41	13	91	0.097	0.27	-22.09	1.0	4.3	5.3	5.67	0.16	2.9	0.4	1.9	-24.31	7.99	2.9	5.84	
36	Holloway Lane	HL 87 B17	67	39	34	76	0.100	0.26														
37	Holloway Lane	HL 87 B24	5	39	37	63	0.075	0.34	-22.81	0.2	1.4	7.9		0.05	41.6	0.1	0.1					
38	Holloway Lane	HL 87 B45	7	36	29	78	0.088	0.21														
39	Holloway Lane	HL 87 B67	25	53	4	94	0.085	0.23	-21.32	1.0	4.3	4.9	4.95	0.18								
40	Holloway Lane	HL 82 III 42	10	30	8	76	0.084	0.21	-21.66	1.1	5.0	5.2	4.30	0.19								
41	Holloway Lane	HL 82 III 61	40	38	22	77	0.107	0.31	-20.30	1.0	4.5	5.2	5.78	0.17	1.8	0.1	2.3	-21.72	7.50	3.2		
42	Holloway Lane	WGF 79 41	32	38	11	91	0.090	0.29														
43	Eynesbury	3249 2365	34	47	26	87	0.105	0.21	-16.85	0.1	2.2	35.8	4.44	0.21								
44	Eynesbury	3249 2366	6	43	43	58	0.067	0.30	-11.69	0.0	7.3	0.0	3.97	0.61								
45	Eynesbury	6087 2329	59	30	42	43	0.151	0.34	-19.84	0.1	2.4	21.7	3.88	0.29	7.6	0.0	0.2					

198	Imperial Coll Sports Grd	IMC96 4847B	43	50	35	67	0.098	0.23	-19.61	0.4	2.9	8.5	4.51	0.14								
199	Imperial Coll Sports Grd	IMC96 10358A	44	42	46	55	0.123	0.34														
200	Imperial Coll Sports Grd	IMC96 10358B	15	46	44	64	0.123	0.35	-22.10	0.2	1.9	10.9	4.68	0.12	12.5	0.1	0.1	fail	0			4.02
201	Imperial Coll Sports Grd	IMC96 10358C	62	48	43	63	0.129	0.35														
202	Imperial Coll Sports Grd	IMC96 10358D	48	45	43	62	0.132	0.37	-23.74	0.2	2.0	10.4	7.08	0.11								
203	Imperial Coll Sports Grd	IMC96 11151A	62	58	11	93	0.105	0.27														
204	Imperial Coll Sports Grd	IMC96 11151B	60	50	29	64	0.106	0.36	-21.41	2.5	8.4	3.9	3.76	0.22	5.0	0.3	2.6	OK	3	-22.29	7.95	3.2
205	Imperial Coll Sports Grd	IMC96 1153	54	60	14	90	0.098	0.24	-20.86	0.6	3.4	7.0	6.10	0.16								
206	Cleveland Farm	W257 1149A	47	32	54	28	0.119	0.27	-20.67	0.2	3.7	19.3	3.99	0.23	0.0	0.0	0.0	fail	0			
207	Cleveland Farm	W257 1149B	43	36	40	47	0.130	0.30	-21.56	0.2	4.2	22.6	5.26	0.25								
208	Cleveland Farm	W257 1149C	62	37	40	20	0.125	0.24	-21.85	0.5	5.1	11.1	3.89	0.23								
209	Cleveland Farm	W257 1149D	62	32	55	26	0.130	0.28														
210	Cleveland Farm	W257 1149E	64	35	63	32	0.117	0.25	-20.98	3.7	12.0	3.8	3.99	0.25	0.2	0.1	2.9	OK	3	-22.29	7.10	3.28
211	Cleveland Farm	W257 1149F	42	32	57	35	0.119	0.33														
212	Cleveland Farm	W257 1149G	50	35	35	19	0.112	0.27	-19.60	1.5	5.9	4.7	4.03	0.21	0.3	0.0	1.0	OK	3	-21.60	4.11	3.3
213	Cleveland Farm	W257 1149H	70	28	50	25	0.126	0.32	-21.41	1.3	6.4	5.9	4.31	0.24	0.5	1.5	1.5	OK	3	-21.70	4.01	3.3
214	Cleveland Farm	W257 7000A	45	45	29	89	0.107	0.35	-23.89	0.4	4.1	11.9	4.62	0.17	19.5	0.4	0.0	fail	0			
215	Cleveland Farm	W257 7000B	55	28	22	47	0.107	0.35														
216	Cleveland Farm	W257 7000C	53	31	47	58	0.116	0.39	-22.26	0.8	5.2	7.5	4.23	0.26								
217	Cleveland Farm	W257 7000D	60	42	46	75	0.114	0.39														
218	Cleveland Farm	W257 7000E	70	36	40	75	0.112	0.28	-16.81	0.2	3.1	19.5	3.76	0.26	0.0	0.0	0.0	fail	0			
219	Cleveland Farm	W257 7000F	43	35	33	85	0.134	0.34														
220	Cleveland Farm	W257 7000G	53	29	36	57	0.117	0.48	-24.13	0.5	4.5	9.9	6.66	0.21								
221	Cleveland Farm	W257 7000H	57	33	41	72	0.145	0.27														
222	Cleveland Farm	W257 7000J	53	27	25	48	0.140	0.36	-22.25	0.3	4.2	17.4	4.11	0.24	12.6	0.2	0.0	fail	0			
223	Cleveland Farm	W257 7000K	70	27	25	46	0.126	0.25	-20.68	0.4	4.0	12.4	4.40	0.27								
224	Cleveland Farm	W257 8000A	45	35	30	56	0.113	0.34	-20.40	2.0	7.7	4.4	3.97	0.22	8.1	1.3	2.4	OK	3	-22.03	7.83	3.2
225	Cleveland Farm	W257 8000B	50	31	35	47	0.106	0.28														
226	Cleveland Farm	W257 8000C	39	45	19	92	0.119	0.35	-23.44	1.3	6.2	5.6	4.30	0.25	24.5	0.8	0.0	fail	0			3.85
227	Cleveland Farm	W257 8000D	60	26	37	51	0.105	0.27	-20.22	0.8	4.2	6.3	5.33	0.21								
228	Cleveland Farm	W257 8000E	57	41	18	64	0.111	0.41	-20.96	1.1	6.0	6.3	4.04	0.24								
229	Cleveland Farm	W257 8000F	50	44	38	89	0.121	0.24														
230	Cleveland Farm	W257 8000G	67	35	38	65	0.115	0.20	-20.42	0.2	3.5	23.3	3.78	0.24	0.3	0.0	0.0	fail	0			
231	Cleveland Farm	W257 8000H	53	39	44	78	0.120	0.30														
232	Cleveland Farm	W257 8000J	49	34	49	67	0.113	0.31	-21.61	1.3	6.3	5.6	4.58	0.24								
233	Cleveland Farm	W257 8000K	58	32	50	70	0.115	0.30														
234	Kingsmead Quarry	H54635 1980A	40	31	34	51	0.114	0.26	-20.84	1.0	4.7	5.5	4.09	0.22	0.4	0.0	1.4	OK	1	-22.41	8.11	3.3
235	Kingsmead Quarry	H54635 1980B	53	46	42	71	0.107	0.25	-21.45	0.3	2.5	11.1	4.71	0.19								
236	Kingsmead Quarry	H54635 1980C	50	54	22	83	0.106	0.24	-18.92	0.2	2.7	14.7	4.67	0.16								
237	Kingsmead Quarry	H54635 1980D	32	47	35	66	0.147	0.31	-21.18	0.2	3.1	19.4	6.39	0.20								
238	Kingsmead Quarry	H54635 1980E	47	46	45	58	0.118	0.32	-19.82	0.2	2.5	15.6	4.50	0.18								
239	Kingsmead Quarry	H54635 2348A	53	48	35	80	0.134	0.25														
240	Kingsmead Quarry	H54635 2348B	57	32	59	75	0.120	0.31	-18.19	0.1	2.4	34.3	3.75	0.25	7.9	0.0	0.0	fail	0			
241	Kingsmead Quarry	H54635 2348C	65	31	53	84	0.135	0.24	-16.76	0.1	2.9	36.7	4.47	0.23								
242	Kingsmead Quarry	H54635 2348D	57	30	59	75	0.138	0.27	-18.42	0.1	2.2	28.5	3.57	0.26								
243	Kingsmead Quarry	H54635 2348E	59	31	64	73	0.136	0.27														
244	Kingsmead Quarry	H54635 2545A	39	31	59	71	0.139	0.30	-18.61	0.1	1.9	29.5	3.98	0.25	22.7	0.0	0.0	fail	0			
245	Kingsmead Quarry	H54635 2545B	57	35	60	75	0.130	0.20														
246	Kingsmead Quarry	H54635 2545C	23	30	54	65	0.151	0.27	-18.50	0.1	1.9	30.2	3.86	0.22								
247	Kingsmead Quarry	H54635 2545D	58	32	71	51	0.130	0.28	-20.69	0.1	2.3	42.1	4.34	0.23								
248	Kingsmead Quarry	H54635 2545E	38	35	63	60	0.140	0.36	-20.23	0.1	1.8	24.1	4.40	0.21								

249	Kingsmead Quarry	H54635 3824A	65	34	41	78	0.139	0.21	-20.74	0.1	3.2	34.7	3.78	0.26	3.8	0.0	0.0	fail	0					
250	Kingsmead Quarry	H54635 3824B	65	36	37	86	0.144	0.23	-23.98	0.1	2.9	27.1	4.70	0.23										
251	Kingsmead Quarry	H54635 3824C	50	36	44	80	0.163	0.41	-19.66	0.2	4.7	37.0	3.95	0.24										
252	Kingsmead Quarry	H54635 3824D	65	33	38	81	0.125	0.31	-22.50	0.1	2.7	32.4	5.52	0.25										
253	Kingsmead Quarry	H54635 3824E	60	34	38	76	0.171	0.37	-20.98	0.1	3.2	37.3	4.03	0.27	4.0	0.0	0.0	fail	0					
254	Kingsmead Quarry	H54635 3850A	63	33	36	89	0.168	0.31																
255	Kingsmead Quarry	H54635 3850B	60	37	23	90	0.161	0.43																
256	Kingsmead Quarry	H54635 3850C	60	41	17	93	0.143	0.23	-17.55	0.1	3.0	35.4	3.61	0.24										
257	Kingsmead Quarry	H54635 3850D	60	36	42	73	0.131	0.27	-18.73	0.0	2.2	51.6	3.85	0.26										
258	Kingsmead Quarry	H54635 3850E	60	39	30	90	0.146	0.24	-19.69	0.1	3.1	34.1	3.61	0.24	1.0	0.0	0.0	fail	0					
259	Kingsmead Quarry	H54635 7255A	54	46	37	65	0.145	0.29																
260	Kingsmead Quarry	H54635 7255B	19	50	28	74	0.161	0.31	-20.68	0.1	2.6	27.5	4.34	0.19										
261	Kingsmead Quarry	H54635 7255C	50	48	42	54	0.162	0.28																
262	Kingsmead Quarry	H54635 7255D	55	44	49	53	0.186	0.32	-24.26	0.2	2.1	16.4	5.88	0.18	16.1	0.0	0.0	fail	0				3.92	
263	Kingsmead Quarry	H54635 7255E	5	42	54	41	0.148	0.23	-19.38	0.1	2.5	29.4	4.59	0.19										
264	RMC Land, Harlington	SIE00 876A	53	49	12	92	0.107	0.27	-21.10	1.1	4.6	4.7	3.94	0.17	0.7	0.0	0.1	fail						
265	RMC Land, Harlington	SIE00 876B	48	47	8	93	0.118	0.27	-22.79	1.2	4.7	4.6	5.66	0.17										
266	RMC Land, Harlington	SIE00 876C	38	43	31	63	0.122	0.30	-20.58	1.0	4.5	5.4	5.73	0.12	9.3	0.2	1.5	OK	3		-21.22	6.96	3.2	
267	RMC Land, Harlington	SIE00 876D	48	45	28	89	0.131	0.25																
268	RMC Land, Harlington	SIE00 876E	63	39	43	75	0.116	0.27	-20.49	1.0	4.4	5.3	4.60	0.14										
269	RMC Land, Harlington	SIE00 877A	47	49	16	85	0.114	0.28																
270	RMC Land, Harlington	SIE00 877B	39	52	10	93	0.110	0.31	-21.53	1.2	5.0	4.7	4.12	0.17	0.3	0.0	0.0	fail	0					
271	RMC Land, Harlington	SIE00 877C	68	40	23	75	0.124	0.33	-23.76	1.5	5.2	4.2	4.95	0.18										
272	RMC Land, Harlington	SIE00 877D	43	56	6	95	0.119	0.24	-19.73	0.9	4.8	6.0	4.91	0.16										
273	RMC Land, Harlington	SIE00 877E	35	50	14	86	0.118	0.33																
274	RMC Land, Harlington	SIE00 1301A	58	45	18	92	0.102	0.25	-21.38	0.6	3.1	6.2	4.82	0.15	0.2	0.0	0.0	fail	0					
275	RMC Land, Harlington	SIE00 1301B	50	58	11	88	0.115	0.23	-22.83	0.6	3.1	6.2	6.18	0.12	0.9	0.0	1.3	OK	3		-21.31	6.91	3.2	
276	RMC Land, Harlington	SIE00 1301C	59	54	8	90	0.113	0.23	-20.33	0.4	3.0	9.8	5.65	0.13										
277	RMC Land, Harlington	SIE00 1301D	38	63	10	75	0.093	0.23	-19.65	0.3	2.7	10.5	5.47	0.12										
278	RMC Land, Harlington	SIE00 1301E	50	50	13	91	0.118	0.27	-20.69	0.8	4.1	6.2	6.08	0.13	0.4	0.0	2.2	OK	3		-21.58	8.10	3.2	
279	RMC Land, Harlington	SIE00 2741A	58	45	27	92	0.120	0.29																
280	RMC Land, Harlington	SIE00 2741B	57	50	20	91	0.115	0.31	-21.30	2.0	6.8	3.9	3.84	0.22	0.2	0.0	0.5	fail	1		-21.48	6.95	3.2	
281	RMC Land, Harlington	SIE00 2741C	70	40	27	48	0.122	0.33	-20.07	1.1	4.9	5.3	5.25	0.20	0.3	0.0	2.1	OK	3		-21.57	7.65	3.3	
282	RMC Land, Harlington	SIE00 2741D	58	46	26	90	0.104	0.28	-18.91	0.7	3.9	6.7	4.67	0.19										
283	RMC Land, Harlington	SIE00 2741E	60	44	28	85	0.109	0.24																
284	RMC Land, Harlington	SIE00 2742A	55	60	2	98	0.110	0.30	-21.14	1.4	5.4	4.4	3.81	0.21	1.5	0.0	0.1	fail	0					
285	RMC Land, Harlington	SIE00 2742B	67	42	27	73	0.108	0.34	-22.87	2.0	6.4	3.7	4.49	0.19										
286	RMC Land, Harlington	SIE00 2742C	58	55	5	96	0.109	0.22	-19.36	0.9	4.5	5.9	6.10	0.18	1.3	0.0	2.6	OK	3		-21.58	8.27	3.2	
287	RMC Land, Harlington	SIE00 2742D	31	45	7	96	0.098	0.23	-19.25	0.6	3.3	6.6	5.34	0.14										
288	RMC Land, Harlington	SIE00 2742E	53	39	16	86	0.105	0.26	-21.30	1.4	5.3	4.5	3.90	0.16	0.5	0.0	0.1	fail					4.89	
289	RMC Land, Harlington	SIE00 3921A	18	41	16	92	0.080	0.30																
290	RMC Land, Harlington	SIE00 3921B	5	44	28	93	0.119	0.31	-21.75	0.4	2.5	7.2	-	-	27.2	0.1	0.0	fail	0					
291	RMC Land, Harlington	SIE00 3921C	38	67	4	98	0.111	0.15	-19.07	0.2	2.3	16.1	6.39	0.13										
292	RMC Land, Harlington	SIE00 3921D	58	41	34	90	0.138	0.34	-19.91	0.3	2.4	8.9	4.92	0.15	13.1	0.0	0.0	fail	0					
293	RMC Land, Harlington	SIE00 3921E	43	40	33	86	0.116	0.23																
294	Haddenham CE	C540.839.60	40	40	29	89	0.114	0.26	-18.61	0.1	2.0	20.7	6.24	0.16										
295	Haddenham CE	C391D	49	38	26	79	0.145	0.24	-20.75	0.1	2.5	20.4												
296	Haddenham CE	C474D	37	40	31	58	0.133	0.24	-22.41	0.1	2.3	24.0	5.08	0.19	18.9	0.0	0.0	fail	0					
297	Haddenham CE	C475D	50	56	36	46	0.100	0.28	-19.90	0.1	1.6	13.4	5.26	0.17										
298	Haddenham CE	C3965K	67	37	36	89	0.126	0.24	-21.79	0.1	3.6	29.2	4.36	0.21										

Appendix III: Data (amino-acid ratios)

ID	Site	Site ID	AMINO ACID ANALYSIS															
			Asp	Glu	Ser	Gly	Thr	Ala	Arg	Tyr	Val	Met	Phe	Ile	Leu	Lys	ohP	Pro
			Mole %															
35	Holloway Lane	HL 87 B66	4.2	8.8	3.6	31.6	1.9	11.9	5.5	0.1	2.5	0.3	1.4	1.3	2.6	2.8	9.7	11.7
99	Berinsfield	BERWC74 Grave 1	4.6	8.5	3.7	25.7	2.2	12.5	6.3	0.1	3.2	0.6	1.6	1.3	3.0	3.0	10.8	12.9
107	Berinsfield	BERWC74 Grave 28	4.4	9.0	3.8	28.1	2.1	11.9	6.0	0.2	3.1	0.5	1.5	1.3	2.9	3.1	9.9	12.4
117	Berinsfield	BERWC74 Grave 92	4.3	9.2	3.4	32.1	1.9	11.8	5.7	0.0	2.8	0.3	1.3	1.1	2.6	2.7	9.3	11.5
126	Berinsfield	BERWC74 Grave 148	4.1	8.8	3.4	30.4	1.9	11.7	5.9	0.1	2.9	0.4	1.3	1.1	2.6	2.9	10.1	12.4
127	Berinsfield	BERWC74 Grave 149	3.9	8.7	3.4	32.0	1.8	12.3	5.6	0.0	2.9	0.3	1.2	1.0	2.3	3.3	9.6	11.8
131	Huntsman's Quarry	HWCM 21698 1103 Bag 2	4.3	9.0	4.0	31.9	1.8	10.9	5.7	0.1	2.4	0.1	1.4	1.3	2.7	3.1	9.5	11.8
159	Bestwall Quarry	BQ98G (55)	4.3	8.8	3.5	27.9	1.9	11.5	6.2	0.2	2.5	0.1	1.5	1.4	2.9	3.6	10.6	13.0
162	Bestwall Quarry	BQ99G (525)	4.4	9.1	3.4	28.8	1.9	11.8	5.9	0.2	2.7	0.0	1.4	1.3	2.7	3.2	10.5	12.6
165	Bestwall Quarry	BQ99H (88)	4.3	8.9	4.1	30.8	2.0	11.1	5.8	0.2	2.3	0.4	1.4	1.2	2.5	2.2	10.3	12.3
166	Bestwall Quarry	BQ99H (427)	4.1	9.0	3.5	29.5	2.1	11.1	5.9	0.2	2.7	0.5	1.5	1.2	2.8	3.1	10.3	12.5
178	Efton CE	B16299	4.2	9.4	3.3	30.2	1.9	11.2	5.8	0.2	2.7	0.2	1.5	1.1	2.7	2.8	10.1	12.8
179	Efton CE	B16300	4.2	9.5	3.5	31.7	1.8	11.2	5.5	0.2	2.6	0.1	1.4	1.1	2.6	2.6	9.6	12.3
182	Efton CE	B14826	0.8	0.0	6.7	24.7	1.7	6.9	3.0	2.0	1.9	7.8	1.1	5.1	7.3	15.2	5.6	10.3
210	Cleveland Farm	W257 1149E	4.3	9.1	4.0	28.9	1.9	11.1	6.1	0.3	2.5	0.2	1.5	1.4	2.9	3.0	10.2	12.6
234	Kingsmead Quarry	H54635 1980A	4.3	9.7	3.7	29.1	1.9	11.1	6.2	0.1	2.5	0.1	1.3	1.3	2.8	3.4	10.7	11.9
266	RMC Land, Harlington	SIE00 876C	4.2	9.2	3.3	28.8	1.9	11.9	6.0	0.1	2.6	0.0	1.4	1.3	2.5	3.3	11.0	12.7
280	RMC Land, Harlington	SIE00 2741B	4.4	9.3	4.1	30.5	1.9	10.9	6.1	0.2	2.4	0.1	1.4	1.2	2.6	2.2	10.1	12.7
281	RMC Land, Harlington	SIE00 2741C	4.6	9.4	3.4	28.6	1.9	11.1	6.1	0.1	2.8	0.0	1.6	1.4	3.0	3.0	10.5	12.6
286	RMC Land, Harlington	SIE00 2742C	4.3	9.2	3.7	28.6	1.9	11.2	6.1	0.2	2.7	0.0	1.5	1.4	2.8	3.0	10.8	12.8